

Numerical Simulation of Diffusion of Second Messengers cGMP and Ca^{2+} in Rod Photoreceptor Outer Segment of Vertebrates

H. Khanal*, V. Alexiades[†], E. DiBenedetto** and H. Hamm[‡]

*Department of Mathematics, University of Tennessee, Knoxville, TN 37996-1300

[†]Department of Mathematics, University of Tennessee, Knoxville TN 37996-1300
and Oak Ridge National Laboratory, Oak Ridge TN 37831

**Department of Mathematics, Vanderbilt University, Nashville TN 37240

[‡]Department of Pharmacology, Medical Center, Vanderbilt University, Nashville TN 37232

Abstract. A crucial step in the process of phototransduction, whereby light is converted into an electrical response in retinal rod and cone photoreceptors, involves interaction and diffusion of cytoplasmic signaling molecules, termed **second messengers**, in the cytosol. A computational model for the interaction and diffusion of the second messengers (cyclic Guanosine Monophosphate and Calcium) during the activation phase of phototransduction in retinal rod cells is described and results of numerical simulations are presented.

INTRODUCTION

The rod outer segment of vertebrates comprises a stack of equispaced *disc* membranes of thickness about 10 nm and at mutual distance of about 14 nm (for the Salamander).

Each disc is made up of two functionally independent layers of lipidic membrane where proteins are embedded, such as rhodopsin (Rh), the light receptor, G protein (G), also called transducin, and cGMP phosphodiesterase (PDE), the effector. These membrane associated proteins can diffuse on the face of the disc where they are located, but cannot abandon the disc. The lateral membrane of the rod contains cGMP-gated channels of small radius. In absence of light these channels are open and allow a positive influx of sodium and calcium (Ca^{2+}) ions. The space within the rod, and not occupied by the discs, is filled with fluid cytosol, in which cyclic-guanosine monophosphate (cGMP) and Ca^{2+} diffuse.

When a photon is absorbed by a molecule of rhodopsin, located on one of the discs, the rhodopsin becomes activated, and in turn activates any G protein it interacts with. Each of the activated G proteins, is capable of activating one and only one catalytic subunit of PDE on the activated disc, by binding to it upon contact. The bound pair so generated is denoted by PDE*. This cascade takes place only on the activated disc. The next cascade, involving cGMP and Ca^{2+} , takes place in the cytosol.

Active PDE* hydrolyzes cGMP in the cytoplasm, thereby lowering its concentration. The decrease of concentration of the cGMP causes closure of some of the cGMP-gated channels of the plasma membrane, resulting in a lowering of the influx of positive ions, and thus a lowering of the local current J across the outer membrane. Because of the

$\text{Na}^+/\text{K}^+/\text{Ca}^{2+}$ exchanger which continues to remove Ca^{2+} from the cytoplasm, there is a decrease in the calcium concentration, which in turn results in an increase in cGMP production by stimulation of Ca^{2+} -inhibited guanyl cyclase, and thus a consequent reopening of the channels. The same decrease of calcium closes the cycle by causing deactivation of rhodopsin through stimulation of rhodopsin kinase. The latter ceases activating new G protein. Thus PDE^* decays to basal, ending depletion of cGMP.

This cascade is well known and it is supported by a sizable amount of published experimental data [4, 14, 22, 21]. However, despite being one of the best understood *signal transduction* processes, its formal mathematical description, is less developed. The classical methods used to describe signal transduction processes assume a well-stirred aqueous environment, and ordinary differential equations provide solutions which average concentrations within the volume of the cell. Recent investigations [3, 13] suggest that these methods are not adequate to describe the precisely regulated signal transduction processes emanating from these highly localized structures, sometimes called "signalsomes" [3].

We present numerical simulations of the diffusion of the second messengers cGMP and Ca^{2+} in the cytoplasm of the rod outer segment of vertebrates during the activation phase. The simulations build on a mathematical model presented in [1] whose main feature is the inclusion of spatio-temporal variations of the concentration of cGMP and Ca^{2+} . The second messengers cGMP and Ca^{2+} , far from being bulk quantities, are regarded as pointwise functions of space and time. In [1], the existing model of [16], which assumes bulk/lumped quantities of cGMP and Ca^{2+} and based on ordinary differential equations, is extended by incorporating diffusion effects and therefore by giving a pointwise description of the phenomenon by means of evolution partial differential equations. The bulk/lumped source terms are correctly modeled as surface-volume reactions occurring on the faces of the discs where cGMP is hydrolyzed.

The numerical simulations we have performed trace the space-time dependence of cGMP. Since the latter is linked to the current J through the cGMP-gated channels, the same simulation provide the distribution of current as a space-time function defined on the lateral boundary of the rod outer segment. Such a dependence permits us to verify numerically some facts put forth in the biological literature about the spread of a single photon response [5].

MATHEMATICAL MODEL

Geometry of the Domain: The outer segment of a rod receptor can be considered as a right circular cylinder $\tilde{\Omega}$ of height H and radius R_{rod} , housing a vertical stack of N equispaced parallel discs C_i , $i = 1, 2, \dots, N_{\text{disc}}$, each of radius R_{disc} , thickness ϵ , and mutually separated by a distance δ . Each of the discs C_i , $i = 1, 2, \dots, N_{\text{disc}}$, carrying the rhodopsin, is assumed to be a short cylinder, coaxial with the rod $\tilde{\Omega}$, of radius R_{disc} and height $\epsilon \ll H$. The discs C_i are equally spaced, i.e., the upper face of C_i has distance δ from the lower face of C_{i+1} . The first C_1 has distance $\delta/2$ from the lower face of the rod $\tilde{\Omega}$ and the last $C_{N_{\text{disc}}}$ has distance $\delta/2$ from the upper face of the rod. The cytosol, where diffusion of second messengers takes place, is the subset $\Omega \subset \tilde{\Omega}$ not occupied by the

cylinders C_i , i.e., $\Omega = \tilde{\Omega} - \bigcup \bar{C}_i, i = 1, \dots, N_{\text{disc}}$. Cylindrical coordinates (r, z, θ) will be employed. We define $F_i^\pm =$ upper/lower disc faces, $L_i =$ lateral boundary of disc C_i (at $r = R_{\text{disc}}$) and $\partial_o\Omega =$ lateral outer boundary (plasma membrane). We also define σ_i to denote the area of disc C_i , σ_{disc} the total area of the N_{disc} discs, V_{cyto} the volume of the cytosol. We also introduce a geometric parameter d , the volume to area ratio, which is approximately $\delta/2$, thus $d = V_{\text{cyto}}/\sigma_{\text{disc}} \approx \delta/2$.

Basic Equations of the Model: Derivation of the general diffusion equations for the concentrations $[cG]$ of cGMP and $[Ca]$ of Ca^{2+} in the fluid cytosol is based on mass balance in an elementary volume. Since there are no volume-sources for either cGMP or Ca^{2+} in the interior of cytosol, the governing equations for diffusion of the second messengers cGMP and Ca^{2+} in Ω can be expressed as

$$\frac{\partial [cG]}{\partial t} - \nabla \cdot (D_{cG} \nabla [cG]) = 0, \quad \frac{\partial [Ca]}{\partial t} - \nabla \cdot (D_{Ca} \nabla [Ca]) = 0 \quad (1)$$

in Ω , for $t > 0$, where D_{cG} and D_{Ca} are the respective diffusion coefficients (in $\mu\text{m}^2\text{s}^{-1}$).

Initial Conditions: Initially, the concentrations of free $[cG]$ and $[Ca]$ in the cytosol can be taken as uniform at their steady-state (dark) values.

Boundary Conditions for $[cG]$: We assume that a small beam of photons hits a disc C_{i_0} on one of its faces, say for example the lower one. Generation and removal of free cGMP concentration in the cytoplasm occurs through binding phenomena on the lower and upper faces of each of the disc. The axial boundary fluxes for $[cG]$ are zero on L_i (lateral boundary of disc C_i) and on $\partial_o\Omega$ (lateral outer boundary). On the upper and lower faces of disc C_i the flux is given by

$$-D_{cG} \frac{\partial [cG]}{\partial z} \Big|_{F_i^\pm} = \pm \frac{\alpha_{\text{max}} d}{1 + ([Ca]/K_{\text{cyc}})^{m_{Ca}}} \mp k_{\text{hyd}} [\text{PDE}]_s [cG] + \delta_{i_0} k_{\text{hyd}}^* [\text{PDE}^*]_s [cG]. \quad (2)$$

The quantity α_{max} is the maximum rate of synthesis of cGMP by guanylyl cyclase [16, pp. 821]. K_{cyc} is the Ca^{2+} concentration that achieves half of the maximum rate, m_{Ca} is a Hill's constant. Multiplying α_{max} by $d (= V_{\text{cyto}}/\sigma_{\text{disc}})$ converts the volumetric flow rate α_{max} to flux across the disc face. The term $k_{\text{hyd}} [\text{PDE}]_s [cG]$ describes hydrolysis of cGMP by dark-activated PDE, with rate k_{hyd} . Similarly, the last term in (2) describes hydrolysis by light-activated PDE* on activated disc(s) i_0 ($\delta_{i_0} = 1$ only when C_i is an activated disc). $[\text{PDE}]_s$ and $[\text{PDE}^*]_s$ are surface densities of the dark and light activated Phosphodiesterase, related to (volumetric) concentrations via $[\text{PDE}] \cdot d = [\text{PDE}]_s$ and $[\text{PDE}^*] \cdot d = [\text{PDE}^*]_s$.

Boundary Conditions for $[Ca]$: Calcium does not penetrate the disc C_i . We assume that the only calcium fluxes into or out of the cytoplasm are by the cGMP-gated channels and the electrogenic exchanger. The boundary fluxes for $[Ca]$ are zero on L_i (lateral boundary of disc C_i) whereas on $\partial_o\Omega$ (lateral outer boundary)

$$-D_{Ca} \frac{\partial [Ca]}{\partial r} = \frac{1}{\Sigma_{\text{rod}} B_{Ca} \mathcal{F}} \left(J_{\text{ex}} - \frac{1}{2} f_{Ca} J_{cG} \right). \quad (3)$$

Here J_{ex} is the current across the boundary of the rod due to electrogenic exchange, J_{cG} is the current carried by the cGMP-gated channels (at a fixed membrane voltage), B_{Ca}

is buffering power of the cytoplasm for calcium, f_{Ca} is the fraction of cGMP-activated current carried by Ca^{2+} , and \mathcal{F} is Faraday's constant. The circulating currents J_{ex} and J_{cG} are described respectively by the the following Michaelis-Menten and Hill type relations [16, pp. 820-821]

$$J_{ex} = \frac{j_{ex}^{sat}}{1 + K_{ex}/[Ca]}, \quad J_{cG} = \frac{j_{cG}^{max}}{1 + (K_{cG}/[cG])^{m_{cG}}}, \quad (4)$$

where j_{ex}^{sat} is saturation exchange current, j_{cG}^{max} is maximal cG-current and Σ_{rod} is the lateral surface area of the Rod Outer Segment. Dividing the flow rate in (3) by Σ_{rod} , converts it to flux. Thus, the local flow rate across a patch of area A of membrane (with local concentrations $[cG]$, $[Ca]$) is given by A times the right-hand side of (3). The total circulating current (J) is the sum $J_{cG} + J_{ex}$.

Activation of PDE: In lieu of a detailed model of the rhodopsin to PDE* cascade taking place on activated discs, we account for the activated PDE by expressing the surface density $[PDE^*]_s$ as a gaussian

$$[PDE^*]_s = \frac{P_0}{4\pi D_a(t - t_{on})} \exp\left(-\frac{r^2}{4D_a(t - t_{on})}\right) \quad (5)$$

with standard deviation $\sqrt{4D_a(t - t_{on})}$, where D_a is a diffusivity of activation of PDE by transducin on the disc surface, P_0 is the number of activated PDE* molecules on a disc, and t_{on} is the time at which light strikes the disc. Note that $[PDE^*]_s$ in (5) is also a solution of 2-dimensional diffusion on the disc face, the response to a Dirac delta source of strength P_0 at $r = 0$ and $t = t_{on}$.

NUMERICAL SIMULATIONS

A computational model of the mathematical problem has been developed based on Finite Volume discretization of the partial differential equations and boundary conditions for the axially symmetric case, and implemented in a Fortran program. Due to the intricate geometry of the cytosol, even the axisymmetric problem involves very intensive computations. We parallelized the scheme for distributed memory clusters of multi-processors or heterogeneous networked computers, employing the MPI (Message Passing Interface) library. The numerical solution of the partial differential equations (1) - (3) gives the evolution of the spatial distribution of concentration of cGMP and Ca^{2+} in the cytosol, from which the circulating currents in equations (4) will be computed.

Parameters: For the numerical experiment, representative parameter values are chosen for the outer segment of Salamander rod cells, and are mostly taken from [16, 20, 11]. Outer segment of the Salamander rod was of radius $R_{rod} = 5.515 \mu m$ containing a stack of $N_{disc} = 800$ discs of height $\epsilon = 14$ nm and radius $R_{disc} = 5.5 \mu m$ equally spaced at a distance $\delta = 14$ nm apart. Height of the rod outer segment $H = 22.4 \mu m$. Typical parameters for the whole cell electrical properties for the dark resting state are taken to be $j_{cG}^{max} = 7000 pA$ and $j_{ex}^{sat} = 0.17 pA$ respectively. The values for the rate constants $k_{hyd} = 7 \times 10^{-5} \text{ molecules}^{-1} \mu m^3 s^{-1}$ and $k_{hyd}^* = 0.183 \text{ molecules}^{-1} \mu m^3 s^{-1}$ are

obtained by matching the parameters with those in [16]. The diffusion coefficient for cGMP is estimated to be $D_{cG} \approx 50 \mu\text{m}^2 \text{s}^{-1}$ by comparing literature values [6, 7, 5, 18] of the experimentally measured effective longitudinal diffusion in cytosol. The diffusion coefficient of calcium in cytosol, $D_{Ca} = 15 \mu\text{m}^2 \text{s}^{-1}$, is taken from [15], which accounts for buffering effects. The surface density of PDE molecules present in the disc membrane is $[\text{PDE}]_s = 100 \text{ molecules } \mu\text{m}^{-2}$ [20]. The remaining parameters used in our simulations are as follows: $\alpha_{\text{max}} = 50 \mu\text{Ms}^{-1}$, $B_{Ca} = 45$, $f_{Ca} = 0.17$, $\mathcal{F} = 96500 \text{ C mol}^{-1}$, $K_{cyc} = 0.15 \mu\text{M}$, $K_{cG} = K_{cG, \text{max}} = 32 \mu\text{M}$, $K_{ex} = 1.5 \mu\text{M}$, $m_{Ca} = 2$ and $m_{cG} = 2$. In order to study the kinetic response of the concentration of various enzymes, proteins and calcium in the cytoplasmic membrane, we have to activate the receptor protein rhodopsin by the flash of light. Our model allows control of the boundary source terms for [cG] in equation (2) in various ways: activation of PDE molecules, with specific strength P_0 and spread rate D_a , over an arbitrary surface area of either of the faces of any desired number of discs, for any specified duration of time, constantly, or on and off.

Activated PDE: We want the entire disc to be activated within a certain time interval $[0, T]$. Since three standard deviations (s.d.) contains 99% of the gaussian in equation (5), we want 3 s.d. $\approx R_{\text{disc}}$ at time T , hence $D_a = R_{\text{disc}}^2 / (36T) \mu\text{m}^2 \text{s}^{-1}$. Thus, for $T = 1$ sec, $D_a \approx 1 \mu\text{m}^2 \text{s}^{-1}$, for $T = 0.1$ sec, $D_a \approx 8 \mu\text{m}^2 \text{s}^{-1}$.

One photon is expected to activate about 1000 molecules of PDE* (1 photon $\rightarrow 1 R^* \rightarrow 10^2 - 10^3 T^* \rightarrow 10^2 - 10^3 \text{ PDE}^*$, see [9]). Thus, a flash delivering Φ photoisomerizations to the rod is expected to activate about 1000Φ PDE molecules. Each activated disc contains $[\text{PDE}]_s \cdot \sigma_{i_0}$ PDE molecules, therefore the number of activated discs $N_{\text{active}} = 1 + 1000\Phi / ([\text{PDE}]_s \sigma_{i_0})$. Distributing the 1000Φ equally among the N_{active} discs, we have $P_0 = 1000\Phi / N_{\text{active}} =$ number of PDE* molecules on each activated disc.

Steady-state: With the input of the above mentioned parameter values, we obtain the dark steady state solution as $[\text{cG}]_{\text{dark}} = 2.91 \mu\text{M}$ and $[\text{Ca}]_{\text{dark}} = 0.60 \mu\text{M}$. This is slightly less than the Nikonov, Lamb, and Pugh [16] dark values of 3 and 0.64. By taking $K_{cyc} = 0.165$, we find the more agreeable values of 2.99 and 0.65. We used these values as the initial conditions for concentrations. The dark standing currents are computed using these values in (4) and are used as normalizing factors for the total circulating currents.

Histories and Profiles: At desired intervals, concentrations and current histories at selected locations in the cytosol and concentration/current profiles along the axial and radial direction were outputted. The plots are drawn in terms of relative and relative responses normalized by their dark values. Some of the results of numerical simulations (with a very coarse mesh of 8 nodes radially and 8 axially, per disc unit) are presented in Fig. 1. and Fig. 2.. The cGMP concentration behaves like the current and it is not presented.

Computations were performed on Compaq AlphaServer SC clusters at Oak Ridge National Laboratory. A typical 1000 msec simulation with 800 discs takes about 1 hr : 20 min using 21 processors.

Conclusion: The form of cGMP and Ca^{2+} concentrations and the light-induced reduction in standing current in the outer segment of a rod predicted from the numerical simulation show a good match to the general trend of the available experimental data. Thus, the simulations will be helpful for interpretation of available biological data,

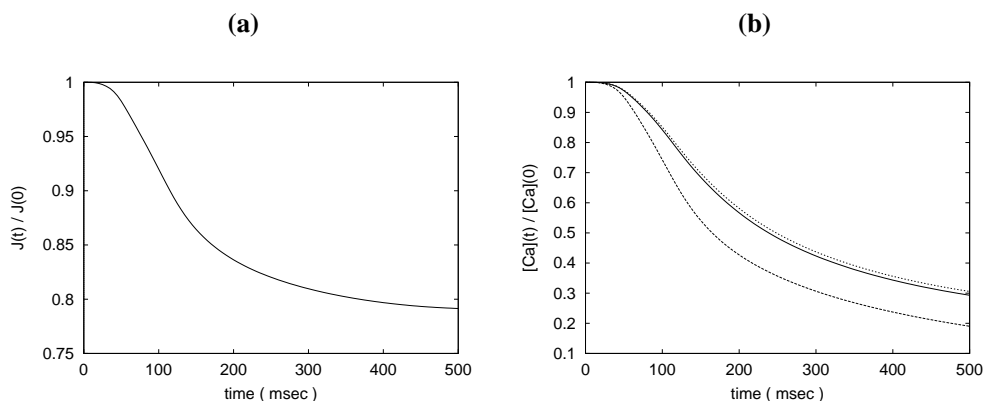


FIGURE 1. Histories of total relative response $J(t)/J(0)$ and calcium relative concentration $[Ca](t)/[Ca](0)$ at some fixed location on the cytosol in the vicinity of the activated disc illustrating the light-induced reduction in standing current and concentration. This simulation was performed for a “truncated” rod with 400 discs (i.e., half of the usual size of a typical Salamander photoreceptor rod) activating 51 discs (# 175 - 225) with about 9285 PDE* molecules per disc via gaussian source of equation (5). The normalizing factors $J(0)$, the total circulating current in the dark steady-state is 65.88 pA and $[Ca](0)$, the concentration of calcium in the dark is 0.65 μ M. **(a)** Relative response $J(t)/J(0)$ versus time. The current reduces 20% by 400msec. **(b)** Relative calcium concentration $[Ca](t)/[Ca](0)$ versus time at three specified locations in the cytosol is shown. The upper two curves are from disc units # 174 and # 226. The lower curve is from disc # 200. The plot shows that the calcium concentration is depleted by more than 50% in the first 200msec.

comparison of model predictions with measurements, determination of sensitivity of output on various model parameters, and to design further biological experiments.

ACKNOWLEDGMENTS

Access to the Compaq AlphaServerSC computer was provided by the Center for Computational Sciences at Oak Ridge National Laboratory and the Evaluation of Early Systems research project, sponsored by the Office of Mathematical, Information, and Computational Sciences, Office of Science, U.S. Department of Energy under Contract No. DE-AC05-00OR22725 with UT-Battelle, LLC.¹ Oak Ridge National Laboratory is managed by UT-Battelle, LLC for the United States Department of Energy under Contract No. DE-AC05-00OR22725.

¹ The U.S. Government retains a non-exclusive, royalty-free license to publish or reproduce the published form of this contribution, or allow others to do so, for U.S. Government purposes.

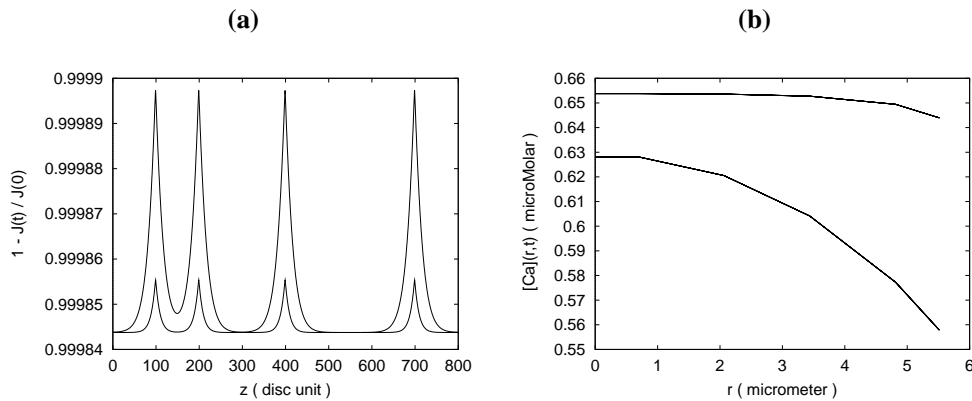


FIGURE 2. Axial (z -direction) and radial (r -direction) profiles at times 150 msec and 600 msec. This simulation was performed with total number of 800 discs (i.e., full size of a typical Salamander photoreceptor rod) activating only four discs (# 100, 200, 400 and 700) with 5000 PDE* molecules on each disc, via gaussian source of equation (5). **(a)** This describes the spatial variation along the z -direction of the relative response of the total current $1 - J(z,t)/J(z,0)$, where $J = J_{cG} + J_{ex}$. This plot clearly depicts interacting and noninteracting discs. There is separation of the diffusion effect between discs # 400 and # 700 but when the activated discs are closer the responses merge. The spread of the response is about 160 disc units, which amounts to $\approx 4.5 \mu\text{m}$. **(b)** This describes the spatial variation of the concentration of calcium along the radial direction at a fixed z -location (just below the activated disc units) in the cytosol.

REFERENCES

1. Andreucci, D., Bisegna, P., Dibenedetto, P., Hamm, H.E., "Mathematical Model of the Dynamics of Second Messengers in Visual Transduction: Homogenization and Concentrated Capacity", submitted to *Biophysical J.*, (2002).
2. Baylor, D., "How photons start vision", *Proc. Natl. Acad. Sci. USA*, **93**, 560-565 (1996).
3. Bhalla, U.S., Iyengar, R., "Emergent Properties of Networks of Biological Signaling Pathways", *Science*, **283**, 381-387 (1999).
4. Burns, M.C., Baylor, D.A., "Activation, deactivation, and adaptation in vertebrate photoreceptor cells", *Annual Rev. Neurosci.*, **24**, 779-805 (2001).
5. Gray-Keller, M., Denk, W., Shraiman, B., Detwiler, P.B., "Longitudinal Spread of Second Messenger Signals in Isolated Rod Outer Segments of Lizards", *J. Physiol.*, **519.3**, 679-692 (1999).
6. Koutalos, Y., Nakatani, K., Yau, K.-W., "Cyclic GMP Diffusion Coefficient in Rod Photoreceptors Outer Segments", *Biophysical J.*, **68**, 373-382 (1995).
7. Koutalos, Y., Nakatani, K., "Calcium Diffusion Coefficients in Rod Photoreceptors Outer Segments", *Biophysical J.*, **76**, A242 (1999).
8. Koutalos, Y., K., Yau, K.-W., "Regulation of Sensitivity in Vertebrate Rod Photoreceptors by Calcium", *Trends in Neuroscience*, **19**, 73-81 (1996).
9. Kurahashi, T., Gold, G.H., "Ionic Channels Mediating Sensory Transduction", in *Introduction to Cellular Signal transduction*, *, Birkhäuser, Boston, 1990, pp 215-234.
10. Lamb, T.D., "Gain and Kinetics of activation in the G-Protein cascade of phototransduction", *Proc. Natl. Acad. Sci. USA*, **93**, 566-570 (1996).
11. Lamb, T.D., Pugh, E.N., "Amplification and Kinetics of the Activation Steps in Phototransduction", *Biochimica et Biophysica Acta*, **1141**, 111-149 (1993).
12. Lamb, T.D., McNaughton, P. A., Yau, K.-W., "Spatial Spread of Activation and Background Desensitization in Toad Rod Outer Segment", *J. Physiol.*, **318**, 463-496 (1981).

13. Leskov, I.B., Klenchin, V.A., Handy, J.W., Whitelock, G.G., Govardovskii, V.I., Bownds, M.D., Lamb, T.D., Pugh, E.N., Arshavsky, V.Y., "The Gain of Rod Phototransduction: Reconciliation of Biochemical and Electrophysical Measurements", *Neuron*, **27**, 525-537 (2000).
14. Liebman, P.A., Parker, K.R., Dratz, E.A., "The molecular mechanism of visual excitation and its relation to the structure and composition of the rod outer segment", *Annual Rev. Physiol.*, **49**, 765-791 (1987).
15. Nakatani, K., Chen, C., Koutalos, Y., "Calcium Diffusion Coefficient in Rod Photoreceptor Outer segments", *Biophysical J.*, **82**, 728-739 (2002).
16. Nikonov, S., Lamb, T.D., Pugh, E.N., "The Role of Steady Phosphodiesterase Activity in the Kinetics and Sensitivity of the Light-Adapted Salamander Rod Photoresponse", *J. Gen. Physiol.*, **116**, 795-824 (2000).
17. Nikonov, S., Lamb, T.D., Pugh, E.N., "Photo receptor Sensitivity and Kinetics in Light Adaptation", *J. Gen. Physiol.*, **117**, 365-366 (2001).
18. Olson, A., Pugh, E.N., "Diffusion coefficient of cyclic GMP in Salamander Rod outer segments estimated with two fluorescent probes", *Biophysical J.*, **65**, 1335-1352 (1993).
19. Pawson, T., Scott, J.D., "Signaling through scaffold, anchoring, and adaptor proteins", *Science* **278**(5346), 2075-80, (1997).
20. Pugh, E.N., Lamb, T.D., "Phototransduction in Vertebrate Rods and Cones: Molecular Mechanisms of Amplification, Recovery and Light adaptation", in *Molecular Mechanism in Visual Transduction*, edited by D.G. Stavenga, W.J. Degrip, and E.N. Pugh Jr, Elsevier, Amsterdam, 2000, pp. 183-255.
21. Schnapf, J.L., Baylor, D.A., "How Photoreceptor Cells Respond to Light", *Scientific Amer.*, **256**, 40-47 (1987).
22. Wald, G., "The Molecular Basis of Visual Excitation", *Nature*, **219**, 200-207 (1968).